Journal of Structural Geology, Vol. 9, No. 3, pp. 375 to 379
Printed in Great Britain

0191-8141/87 $03.00 + 0.00

Energy balance for large thrust sheets and fault-bend folds

R. T. WILLIAMS

Geology Department, University of South Carolina, Columbia, SC 29208, U.S.A.

(*Received* 30 *June* 1986; *accepted in revised form* 9 *October* 1986)

Abstract—Thrust sheet movement over ramps requires energy because of the frictional resistance and deformation within the fault zone, fault-bend folding at the base and top of the ramp, and changes in the gravitational potential energy because of uplift. To model the energy usage, a kinematic model of a foreland thrust sheet is constructed assuming: (1) the ramp is planar and the flats are parallel to bedding; (2) the fault-bend folds are concentric; (3) thickness is preserved for beds that enter the folds parallel to the basal thrust fault and (4) cross-sectional area is preserved for rocks deformed by folding. Equations for the work done within the fault zone, and during uplift and fault-bend folding are derived by combining the kinematic model with stresses that increase in proportion to depth. The relative amounts of energy consumed by friction along the fault, uplift and fault-bend folding are estimated to be 2.7 : 1 : 0.25 for a ramp angle of 30°. The energy balance for the movement of large thrust sheets thus depends principally upon friction in the fault zone and changes in the gravitational energy.

INTRODUCTION

THE FORMATION of duplexes and other structures found in foreland fold-and-thrust belts requires energy. Mitra & Boyer (1986) estimated the amounts of energy used during duplex formation for initiation and propagation of fractures in the fault zone, frictional resistance to thrusting, shear deformation within the thrust sheet, and uplift. They determined that energy is used principally for internal shear deformation of the thrust sheet and uplift against gravity. Specifically, they calculated values of 5×10^{16} J for work done within the basal thrust zone, as compared to 2.3×10^{17}–6.3×10^{17} J for uplift against gravity and 3×10^{17} J for internal deformation due to fault-bend folding, for particular structures where the thrust sheets are 5 km thick. However, their work calculations are incomplete, because although Mitra & Boyer used the strain energy equation, they considered only those terms which involve the shear stress, and do not take into account the variation of stress with depth in the crust.

The purpose of this paper is to present estimates for the relative amounts of energy consumed during the movement of individual thrust sheets by friction in the fault zone, uplift against gravity, and shear deformation in fault-bend folds. The estimates are based on stylized kinematic models of thrusting and concentric fault-bend folds. It is also shown that useful estimates of the amount of energy required for fault-bend folding can be made from the ramp angle and amount of work done against gravity.

WORK DONE IN A FAULT-BEND FOLD

A thrust sheet passing through a fault-bend fold (Suppe 1983) undergoes internal deformation, which irreversibly converts mechanical energy into heat. This work is done by surface forces acting on individual parcels of rock which experience shear deformation. The general form of the work equation is given by Frederick & Chang (1972, p. 129):

$$\dot{W} = \int_V \sigma_{ij,i} q_j - \sigma_{ij} q_{j,i} \, dV, \qquad (1)$$

where $\dot{W}$ is the rate at which work is done within the volume of rock (V) occupied by the fold, σ_{ij} is the stress tensor, and q_j is a velocity vector which represents the rate and direction at which a parcel of rock moves through the fault-bend fold. The sign convention that compressive stress is negative is followed here. The symbol $(,i)$ denotes the partial derivative with respect to the i coordinate, either x or z, as shown in Fig. 1. No explicit assumptions about the rheology of the rocks in the thrust sheet are made during the formulation of equation (1). Instead rheology is accounted for implicitly since it ultimately governs the stresses which develop.

Each term on the right side of equation (1) must be specified in order to calculate the work. The velocity vector of q_j is dependent on the displacement paths through the fold. Mitra & Boyer (1986) follow Suppe (1983) and use straight-line segments to describe the trajectory of the thrust sheet through the fault-bend fold. In this discussion, smooth curves are used instead for the fold hinges, for two reasons: (1) even very tight folds observed in the field remain arcuate, unless a fault disrupts the continuity of bedding; and (2) straight-line segments result in a mathematical singularity in the work equation. This singularity arises because a parcel of rock moving smoothly through the fold instantaneously changes its direction and undergoes infinite vertical acceleration at the hinge, if straight-line segments are used for the displacements, although this approximation may be satisfactory in calculations of bed lengths and areas for balancing cross-sections.

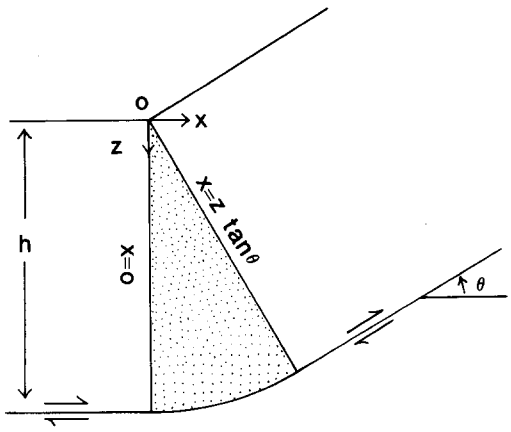

Fig. 1. Fault–bend fold geometry and coordinate system definition. x and z are the horizontal and vertical coordinate axes, respectively, with origin at 0, h is the thickness of the thrust sheet and θ is the ramp angle. Fault–bend folding occurs in the stippled region at the base of the ramp, bounded by lines $x = 0$ and $x = z \tan \theta$.

Use of the work equation does not limit the kinds of deformation that can be considered, except that accelerations must remain finite. For the purpose of this discussion it is assumed that fault–bend folding preserves both area in cross-section and the thickness for beds which enter the fold parallel to the basal thrust fault. In the case of concentric fault–bend folds the components of the velocity vector q_j are

$$q_x = \frac{z}{(x^2 + z^2)^{1/2}}\,\dot{u}$$
$$q_z = -\frac{x}{(x^2 + z^2)^{1/2}}\,\dot{u} \tag{2}$$

where $\dot{u}$ is a constant which represents the rate at which the thrust sheet advances. These equations apply within the region occupied by the fold. If the step-up angle is θ, then the fold lies between the lines $x = 0$ and $x = z \tan \theta$ as shown in Fig. 1.

Estimating σ_{ij} is more problematic. Mitra & Boyer (1986) specified only the shear stress, and assumed that its value is constant:

$$\sigma_{xz} = \sigma_{zx} = \tau. \tag{3}$$

Initially, I will make the same assumption here. Using the displacements given by (2) and the stresses given by (3) the work equation (1) becomes

$$\frac{\dot{W}}{\dot{u}} = \tau \int_{z=0}^{h} \int_{x=0}^{z \tan \theta} \frac{x^2 - z^2}{(x^2 + z^2)^{3/2}}\,dx\,dz \tag{4}$$

where h is the thickness of the thrust sheet (Fig. 1). In this equation and those that follow it is to be understood that the work calculated is per kilometer of thrust sheet width, because the integration is taken over the area in cross-section. Performing the integrations yields

$$\frac{\dot{W}}{\dot{u}} = h\tau\left(-2 \sin \theta + \log_e \frac{1 + \sin \theta}{\cos \theta}\right). \tag{5}$$

This result is substantially the same as that obtained by Mitra & Boyer (1986, Appendix) which is

$$\frac{\dot{W}}{\dot{u}} = -2h\tau \tan \frac{\theta}{2}. \tag{6}$$

For example, the ratio of equation (5) to (6) is 0.98 and 0.83, for $\theta = 10°$ and 30°, respectively.

The approximation that σ_{ij} is constant is generally not satisfactory for thick thrust sheets, particularly those that carry their overburden with them, and thus extend to the surface where σ_{xz} and σ_{zz} vanish. McGarr (1980) has shown that, for a homogeneous subsurface, the components of stress are linear functions of depth. For the purpose of this discussion, linear functions are used to represent stress components at depth in the thrust sheet. These are viewed as first-order approximations only, because the stress field in the earth depends on many factors, including tectonic forces, overburden weight, possible stress refraction at the boundaries between different structural–lithic units, and stress due to bending these units. The stress within a thrust sheet is approximately given by

$$\sigma_{xx} = A_1 + B_1 z$$
$$\sigma_{zz} = A_2 + B_2 z \tag{7}$$
$$\sigma_{xz} = -\frac{(A_1 - A_2)}{2} \tan 2\gamma - \frac{(B_1 - B_2)}{2} \tan 2\gamma z$$

where A_1, A_2, B_1 and B_2 are constants, A_1 and A_2 are the normal components of stress at $z = 0$ (Fig. 1), and B_1 and B_2 are the stress gradients. The angle γ is the inclination of the principal stress direction with respect to the x-axis.

The work done in this stress field is obtained by evaluating the work equation (1) for the displacements and stresses given in equations (2) and (7), respectively. The result is

$$\frac{\dot{W}}{\dot{u}} = \left[\cos \theta - 1 + \frac{\tan 2\theta}{2} \times \left(2 \sin \theta - \log_e \frac{1 + \sin \theta}{\cos \theta}\right)\right](A_1 - A_2)h + \frac{\tan 2\gamma}{2}\left(\sin \theta - \log_e \frac{1 + \sin \theta}{\cos \theta}\right)(B_1 - B_2)h^2 - \frac{1}{2}\left(B_1(1 - \cos \theta) + B_2 \times \frac{(2 - 2 \cos \theta - \sin^2 \theta)}{\cos \theta}\right)h^2. \tag{8}$$

The relative importance of work done within the fault–bend fold in the overall energy balance can be judged by comparing this result to the change in gravitational potential energy. This comparison may be illustrated by consideration of two examples (Fig. 2). Example I involves a long thrust sheet which continues to advance for an indefinite distance after travelling up the ramp. This kind of thrusting has occurred in the central Appalachian foreland of Virginia and West Virginia (Jacobeen & Kanes 1974). Estimates of the total work done during the emplacement of these thrust

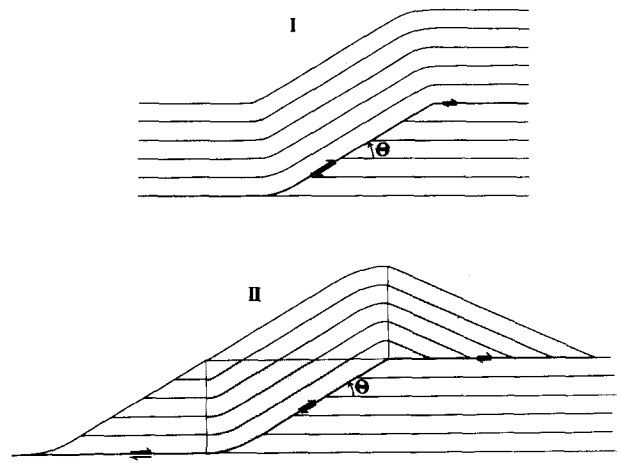

Fig. 2. Two stylized models of thrust sheets. Example I is a ramp–flat structure in which the thrust sheet climbs the ramp and continues to advance indefinitely. Fault-bend folding occurs at the base and top of the ramp. Example II contains a structural culmination at the top of the ramp. Rocks in the patterned region at the top of the ramp occupied the corresponding area along the ramp prior to thrusting. Originally horizontal bedding dips toward the foreland in this part of the structure.

sheets must also take into account the energy required to form a fold having a foreland-dipping limb at the leading edge of the thrust sheet. Example II (Fig. 2) considers the formation of the foreland-dipping limb, and also approximates isolated structures which culminate at the top of the ramp, as in the Sequatchie anticline and the Allegheny structural front in the southern Appalachians (Milici 1968, Milici & Leamon 1975), or individual imbricate slices in duplexes (Boyer & Elliott 1982).

For Example I the amount of rock (area in cross-section) moved from the lower level to the upper level, per unit time, is $h\dot{u}$. Hence the rate at which work is done against gravity is

$$\dot{W}_g = \rho g h^2 \dot{u} \tag{9}$$

where ρ is the density of the rock in the thrust sheet and g is gravity (980 gals). The rate at which work is done within the fold at the base of the ramp is estimated from equation (8), assuming values for the constants as follows: $A_1 = A_2 = 0; B_2 = -\rho g; B_1 = 2B_2$; and $\gamma = 15°$. These values for A_1 and A_2 are appropriate because of the free surface at the top of the thrust sheet, where $\sigma_{zz} = \sigma_{xz} = 0$. The vertical stress gradient is approximately lithostatic, so $B_2 = -\rho g$. The relationship $B_1 = 2B_2$ follows from stress measurements in boreholes in seismically active regions (Zoback & Hickman 1982), and depends on the compressive strength of the rocks at different depths within the stratigraphic column. The value for γ is chosen to produce a shear stress increase of about 7.5 MPa per km of depth. For a 5 km thick thrust sheet this yields an average shear stress equal to the 20 MPa value used by Mitra & Boyer (1986), based on data from the McConnell thrust (Elliott 1976). It is also consistent with estimates of shear stress in the Taiwan foreland (Davis *et al.* 1983) of 65 MPa at 10 km depth, assuming $\rho = 2400$ kgm/m^3. The work term for internal deformation obtained from equation (8) using these values is:

$$\dot{W} = \frac{\rho g}{2}\left[0.58\left(\sin\theta - \log_e \frac{1+\sin\theta}{\cos\theta}\right) + \frac{\sin^2\theta}{\cos\theta}\right] h^2 \dot{u}. \tag{10}$$

This is the contribution from the fault-bend fold at the base of the ramp. It is doubled to approximately account for the effect of the fold at the top of the ramp. The importance of work done by fault-bend folding relative to the change in gravitational potential energy due to uplift is indicated by the ratio obtained from equation (9) and twice equation (10):

$$\frac{\dot{W}}{\dot{W}_g} = 0.58\left(\sin\theta - \log_e \frac{1+\sin\theta}{\cos\theta}\right) + \frac{\sin^2\theta}{\cos\theta} \tag{11}$$

which is 0.03, 0.12 and 0.26 for $\theta = 10°$, 20° and 30°, respectively.

The geometry depicted in Example II (Fig. 2) results from thrusting which is active for a specific time interval, equal to $h(\theta + \cot\theta)/\dot{u}$. Prior to thrusting the thickness of the section is uniform, and the rock contained in the patterned region at the top of the ramp occupies the corresponding area along the ramp. During thrusting, shear strain occurs within the two concentric fault-bend folds at the base and top of the ramp. The work done against gravity in this case is

$$W_g = \frac{\rho g h^3}{12}\left[5(\theta + \cot\theta) + 4(\sin\theta + \operatorname{cosec}\theta)\right]. \tag{12}$$

The work done by internal deformation in Example II includes contributions from each of the two fault-bend folds. The patterned region at the top of the ramp has traversed the upper fold. The portion of the thrust sheet along the ramp has traversed the lower fold. If it is assumed, as in Example I, that the same stresses apply in both folds, then the total work done within the folds is obtained by evaluating equation (10) for these two regions, using $u = h(\theta + \cot\theta)$. The result is

$$W = \frac{3\rho g h^3}{4}\left[0.58\left(\sin\theta - \log_e \frac{1+\sin\theta}{\cos\theta}\right) + \frac{\sin^2\theta}{\cos\theta}\right] \times (\theta + \cot\theta). \tag{13}$$

The ratio $\dot{W}/\dot{W}_g$ for Example II obtained from (12) and (13) is

$$\frac{W}{W_g} = \frac{9\left[0.58\left(\sin\theta - \log_e \frac{1+\sin\theta}{\cos\theta}\right) + \frac{\sin^2\theta}{\cos\theta}\right] \times (\theta + \cot\theta)}{5(\theta + \cot\theta) + 4(\sin\theta + \operatorname{cosec}\theta)} \tag{14}$$

which is 0.03, 0.11 and 0.25 for $\theta = 10°$, 20° and 30°, respectively, and is nearly the same as in Example I.

WORK DONE IN THE FAULT ZONE

The work done along the basal thrust fault can be estimated from the work equation. An alternative form, obtained by applying Green's theorem (Green 1828, Love 1927, p. 85) to equation (1), is appropriate where

the fault zone is very thin relative to the thickness of the thrust sheet. This form, which expresses work in terms of stress and displacement along the footwall instead of their derivatives, is

$$\dot{W} = \int_A \sigma_{ij} n_i q_j \, dA \tag{15}$$

where A represents the area of the fault surface and n_i is a unit vector perpendicular to it. The stress vector $\sigma_{ij}n_i$ acting on the fault depends on the lithostatic stress (ρgh), the increment in stress due to tectonic compression, and the coefficient of friction and fluid pressure in the fault zone. Laboratory measurements of the coefficient of friction (f) using dry rocks place its value in the range $0.6 \leqslant f \leqslant 0.9$ (Byerlee 1977). However, lower values may be appropriate for the large-scale deformations associated with a major thrust fault. Turcotte & Schubert (1982 p. 356) estimate $f = 0.36$ for the Wind River, Wyoming, thrust fault. Sibson (1983) estimated that shear resistance to thrusting in the brittle upper crust is proportional to depth, and increases by about 21 MPa/km, assuming $f = 0.75$ and hydrostatic fluid pressures in the fault zone. Estimates of shear stress by Davis *et al.* (1983) for the Taiwan foreland, and Hatcher & Williams (1986) for large, subhorizontal thrust sheets transported along brittle faults, indicate that the increase in shear resistance with depth is about 7.5 MPa/km, which is consistent with the low coefficient of friction reported by Turcotte & Schubert. Evaluating the integrand of equation (15) using q_j as specified in equation (2) yields

$$\sigma_{ij} n_i q_j = \mu \rho g h \dot{u} \tag{16}$$

where μ is a constant that depends on the average density of the thrust sheet and the coefficient of friction and fluid pressure in the fault zone. Values of μ are low ($\mu = 0.32$) for low (7.5 MPa/km) shear resistance and intermediate densities ($\rho = 2670$ kgm/m^3). Conversely, μ is large ($\mu = 0.8$) for higher (21 MPa/km) estimates of the shear resistance.

The work done within the basal thrust fault zone is estimated for Example II by evaluating the work equation (15) for the integrand given in (16). The length of the thrust fault underlying this thrust sheet is $(2\theta + 2 \cot \theta + \operatorname{cosec} \theta)h$. Hence

$$\dot{W} = \mu \rho g h^2 (2\theta + 2 \cot \theta + \operatorname{cosec} \theta)\dot{u}. \tag{17}$$

Integrating over the time interval that thrusting is active

$$W = \mu \rho g h^3 (\theta + \cot \theta)(2\theta + 2 \cot \theta + \operatorname{cosec} \theta). \tag{18}$$

The work ratio of friction along the thrust fault to uplift for Example II is obtained from the ratio of equation (18) and (12):

$$\frac{W}{W_g} = 12\mu \frac{(\theta + \cot \theta)(2\theta + 2 \cot \theta + \operatorname{cosec} \theta)}{5(\theta + \cot \theta) + 4(\sin \theta + \operatorname{cosec} \theta)} \tag{19}$$

which is 7.3, 3.8 and 2.7 for θ equal to 10°, 20° and 30°, respectively, and $\mu = 0.32$. These values for the ratio (19) are increased by a factor of 2.5 if the larger estimate $\mu = 0.8$ is used. Lower values may be possible if thrusting is not frictional sliding, but rather is dominated by fluid-assisted pressure-solution creep, as described by Wojtal & Mitra (1986).

The amount of work done overcoming friction along the thrust fault in Example I cannot be determined, because the length of the fault is not specified. However, it is clear that the work ratio of friction to gravity exceeds that of Example II, because the fault is longer and the uplift is the same. Hatcher & Williams (1986) suggest that the length of such a thrust sheet is limited by the compressive strength of the rocks it contains. Beyond some critical length, the rocks will not support the tectonic compressive stress required to move the thrust sheet, and the length will be reduced by additional faulting and imbrication.

DISCUSSION

The energy required for thrusting comes from forces related to compressive plate boundaries and topographic slope (Davis *et al.* 1983). The greatest portion of this energy is used to overcome frictional resistance within the fault zone. The amounts of energy used for uplift against gravity and internal deformation due to fault–bend folding depend on the ramp angle, θ, and are estimated to be 37% and 10%, respectively, of the energy consumed within the fault zone for $\theta = 30°$, decreasing as θ decreases. These results apply to structures in which the thicknesses of individual thrust sheets are comparable to the depth of the basal thrust fault, because of the assumptions made here about the way stress varies with depth. The work equation (5) yields the same result as the strain energy equation (6) (Mitra & Boyer 1986) for small shear strains, corresponding to small values of θ. The examples considered here (Fig. 2) involve arbitrary ramp angles.

The equations derived in this paper apply *sensu stricto* only to the bending of thrust sheets as they ride over non-planar fault surfaces, as described by Suppe (1983). Generalizations concerning duplex formation must also take into account the energy consequences of other kinds of folds and deformation within the thrust sheets. It is unlikely that the majority of folds observed in any particular duplex result solely from fault–bend folding. Duplex formation involves deformation within structurally higher and earlier formed thrust sheets (Boyer & Elliott 1982). Folding of these imbricate masses would probably entail more work than that required for a single ramp. In a duplex, beds within one imbricate slice are not necessarily parallel to those within adjacent slices, making difficult the transfer of interbed slip from one imbricate to another.

Work calculations show that imbricate structures including duplexes are stiffened by shear deformation within fault–bend folds. Work is the product of force and displacement; thus for given displacement of a thrust sheet the additional energy utilized for internal deforma-

tion requires greater compressive forces, and consequently greater levels of stress. This effect has previously been examined by treating the thrust sheet as a beam which is bent when it encounters a ramp (Wiltschko 1979). The resistance to thrusting attributable to fault-bend folding is less than 25% of that which arises because of uplift, and less than 10% of the total for $\theta = 30°$. This percentage is dependent upon the stress field in which thrusting occurs.

The conclusion that fault-bend folding requires relatively little work is consistent with observations of the deformation in large thrust sheets. Fault zones commonly show evidence of high energy processes, including the formation of cataclasites, accompanied by intense fracturing and penetrative deformation (House & Gray 1982, Diegal & Wojtal 1985). However, these effects are generally restricted to a narrow band within a few meters of the fault, and are only rarely observed throughout the larger volume of the thrust sheet where the energy used for fault-bend folding is dissipated.

CONCLUSIONS

(1) The energy balance for the transport and emplacement of large thrust sheets can be expressed in terms of tectonic compression, frictional forces along the basal thrust fault and change in gravitational potential energy due to uplift. Most of the energy is used to overcome frictional resistance, including sliding friction and deformation, within the fault zone. The energy for internal deformation of these thrust sheets is a relatively small part of the total. For particular thrust sheets useful estimates of the relative contributions of friction, uplift and internal deformation to the energy balance can be made from measurements of the ramp angles. Mitra & Boyer (1986) have already shown that the energy required for nucleation of the thrust surface and crack propagation is relatively small.

(2) The work equation is preferable to the strain energy equation for energy balance calculations of thrusting and duplex formation. Use of the work equation is limited to problems where the shapes of the ramp and fault-bend folds are represented by smooth curves, which preserve the continuity of velocity and acceleration of a parcel of rock displaced by the thrusting. It does not apply, in general, where only straight lines are used, because these may imply a discontinuity in velocity, and infinite acceleration as the rocks moving through the fold change direction.

(3) Concentric folds are a viable representation of fault-bend folds in foreland fold-and-thrust belts. The question of the relative frequency of occurrence of concentric folds versus other shapes including narrow kink-bands remains unresolved.

Acknowledgements—Portions of this work were supported by National Science Foundation Grant EAR-8417894. Comments by William M. Dunne, Robert D. Hatcher, Jr, Gautam Mitra and an anonymous referee resulted in considerable improvement of the manuscript. The author remains responsible, however, for all errors of fact or interpretation.

REFERENCES

Boyer, S. E. & Elliott, D. 1982. Thrust systems. *Bull. Am. Ass. Petrol. Geol.* **66**, 1196–1230.

Byerlee, J. C. 1977. Friction of rocks, in *Experimental Studies of Rock Friction with Application to Earthquake Prediction* (edited by Evernden, F. G.). U.S. Geological Survey, 55–77.

Davis, D., Suppe, J. & Dahlen, F. A. 1983. Mechanics of fold-and-thrust belts and accretionary wedges. *J. geophys. Res.* **88**, 1153–1172.

Diegel, F. A. & Wojtal, S. F. 1985. Structural transect in SW Virginia and NE Tennessee, in *Studies in Geology* **9** (edited by Woodward, N. B.). University of Tennessee, Department of Geological Sciences, 70–143.

Elliott, D. 1976. The energy balance and deformation mechanisms of thrust sheets. *Phil. Trans. R. Soc. Lond.* **A283**, 289–312.

Frederick, D. & Chang, T. S. 1972. *Continuum Mechanics*. Scientific Publishers, Boston.

Green, G. 1828. *Essay on Electricity and Magnetism*. Nottingham.

Hatcher, R. D., Jr. & Williams, R. T. 1986. Mechanical model for single thrust sheets part I: Taxonomy of crystalline thrust sheets, and their relationships to the mechanical behavior of orogenic belts. *Bull. geol. Soc. Am.* **97**, 975–985.

House, W. M. & Gray, D. R. 1982. Cataclasites along the Saltville thrust, U.S.A. and their implications for thrust sheet emplacement. *J. Struct. Geol.* **4**, 257–268.

Jacobeen, F. & Kanes, W. H. 1974. Structure of the Broadtop synclinorium and its implications for Appalachian structural style. *Bull. Am. Ass. Petrol. Geol.* **58**, 362–375.

Love, A. E. H. 1927. *A Treatise on the Mathematical Theory of Elasticity*, 4th edn. Dover, New York.

McGarr, A. 1980. Some constraints on levels of shear stress in the crust from observations and theory. *J. geophys. Res.* **85**, 6231–6238.

Milici, R. C. 1968. The Allegheny structural front in Tennessee and its regional tectonic implications. *Am. J. Sci.* **268**, 127–141.

Milici, R. C. & Leamon, A. R. 1975. Cranmore Cove–Chattanooga fault system: a model for the structure along the Allegheny front in southern Tennessee. *Geology* **3**, 111–113.

Mitra, G. & Boyer, S. E. 1986. Energy balance and deformation mechanisms of duplexes. *J. Struct. Geol.* **8**, 291–304.

Sibson, R. H. 1983. Continental fault structure and the shallow earthquake source. *J. geol. Soc. Lond.* **140**, 741–767.

Suppe, J. 1983. Geometry and kinematics of fault-bend folding *Am. J. Sci.* **283**, 684–721.

Turcotte, D. L. & Schubert, G. 1982. *Geodynamics*. Wiley, New York.

Wiltschko, D. V. 1979. A mechanical model for thrust sheet deformation at a ramp. *J. geophys. Res.* **84**, 1091–1104.

Wojtal, S. F. & Mitra, G. 1986. Strain hardening and strain softening in fault zones from foreland thrusts. *Bull. geol. Soc. Am.* **97**, 674–687.

Zoback, M. D. & Hickman, S. 1982. In situ study of the physical mechanisms controlling induced seismicity at Monticello reservoir, South Carolina. *J. geophys. Res.* **87**, 6959–6974.